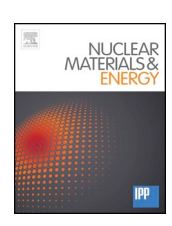
ELSEVIER

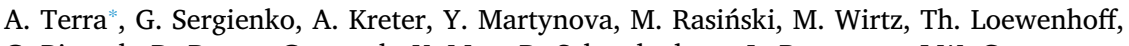
Contents lists available at ScienceDirect

# Nuclear Materials and Energy

journal homepage: www.elsevier.com/locate/nme



# Micro-structured tungsten, a high heat flux pulse proof material



G. Pintsuk, D. Dorow-Gerspach, Y. Mao, D. Schwalenberg, L. Raumann, J.W. Coenen,

S. Brezinsek, B. Unterberg, Ch. Linsmeier

Forschungszentrum Jülich GmbH, Institut für Energie- und Klimaforschung, 52425 Jülich, Germany



#### ARTICLE INFO

Keywords:
Micro-structured tungsten
PFC
PFM
High heat load
Thermal cycling
Retention
Erosion
Emissivity

#### ABSTRACT

Micro structured tungsten is a new approach to address one of the main issues of tungsten as high heat flux (HHF) plasma facing material (PFM), which is its brittleness and its propensity to crack formation under pulsed, ELM like, heat loads (Loewenhoff et al., 2015; Wirtzet al., 2015 [2,3]). With power densities between  $100 \text{ MW/m}^2$  and  $1 \text{ GW/m}^2$ , progressive thermal fatigue induced damages like roughening, subsequent cracking and even melting will occur in dependence on the pulse number and PFM base temperature. This represents a serious issue for the usage of tungsten as HHF-PFM. In future tokamaks, such as ITER, about  $10^8 \text{ ELMs}$  are expected to occur during the operational lifetime.

Several approaches have been tried to overcome this brittleness issue, e.g. alloying tungsten with others elements (Linsmeier et al., 2017 [4]) or introducing pseudo-ductility due to the additions of fibres thus creating composites (Reiser et al., 2017 [5]). Micro-structured tungsten showed a significant improvement in comparison with any of these approaches with respect to the damage expected by ELMs. This investigation on both bulk reference and micro-structured tungsten was performed in the PSI-2 facility (Kreter et al., 2015 [8]). A sequential load was applied combining steady state deuterium plasma (5.1  $\times$  10<sup>25</sup> D + m $^{-2}$ , 51 eV, 240 °C, 150 min) loading with laser pulses (up to  $10^5$  pulses of 0.5 GW/m $^2$ , 3.6 mm spot diameter, 20 J, 1 ms pulse duration, up to 25 Hz pulse frequency). In contrast to reference bulk tungsten, none of the applied loading conditions caused any evident damage on the micro-structured tungsten. The maximum surface temperature within the loaded area measured with a fast pyrometer was increased by about 800 °C at the end of the laser exposure for the reference sample. This is related to the emissivity changes and local temperature increase caused by surface degradation. Meanwhile, the micro-structured sample did not show any change of its temperature response from the 10th to the 100 000th pulse.

## 1. Introduction

Fusion experimental reactors nowadays are mainly turned towards metallic and especially tungsten based plasma-facing components (PFC) at least in high heat flux areas like divertor (while beryllium is foreseen for less loaded areas, at least for ITER). This is due to the number of benefits of tungsten, like high melting point, its low sputtering, moderate hydrogen isotopes retention as limited both co-deposits formation and chemical reactivity with hydrogen, but also its good thermal properties, which are an advantage for proper power exhaust. Its relative stability under neutron irradiation and the transmutation into mostly non-radioactive elements is also a non-negligible advantage. However, tungsten suffers of a major drawback which is its propensity to crack and go under catastrophic failures under repeated heat loads,

especially when loaded under its ductile to brittle temperature (DBTT), which is usually around 300  $^{\circ}$ C [2,3].

Scientific community addressed this problem within several approaches for now several years [4–7], of which most commons are alloying tungsten with other elements and/or controlling its grain microstructure. However, a couple of years ago emerged a new one which is the micro-structuring of the tungsten based PFC. It was first demonstrated an improvement of factor of at least 10<sup>5</sup> over traditional tungsten as plasma facing material in the area of ELMs induced thermal fatigue (considering induced surface damage as evaluation criterion), while not showing any other main concern or drawback in the areas of fuel retention, power handling or erosion [9]. These first results were confirmed later by additional means including *in situ* surface degradation monitoring through temperature and visual aspect (sublimation of

E-mail address: a.terra@fz-juelich.de (A. Terra).

<sup>\*</sup> Corresponding author.

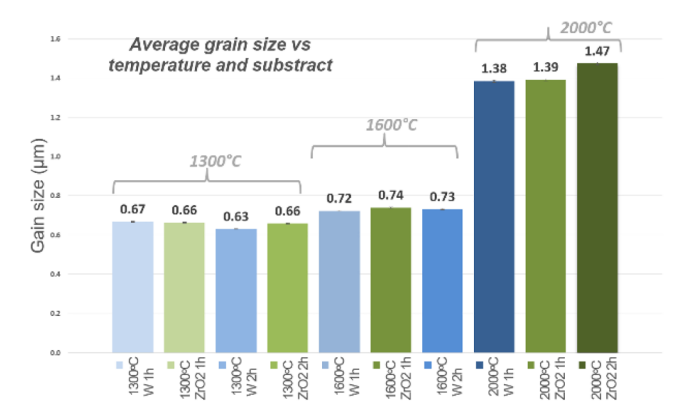


Fig. 1. Average grain size of recrystallized fibres depending on container type, temperature and duration.

previously implemented fuzz), and a  $10^5$  improvement factor could be again observed but also confirmed by means of finite element analysis [10]. In the current paper, we are going to demonstrate that this improvement is still observable even after recrystallization of the base tungsten material.

## 2. Experimental setup

#### 2.1. Samples

The micro-structured samples were prepared in the exact same way as it was previously done [9,10], with about 1500 fibres of Ø150  $\mu$ m diameter (2.4 mm long), potassium doped fibre embedded in an industrial grade copper matrix (Cu-ETP), up to approximately 2/3 of their height, all tight packed and arranged into a compact hexagonal lattice. Each sample, of reference bulk tungsten or micro-structured, offered a 5 by 5 mm surface. However, compared to previous experiments, preliminary to the fabrication of the samples, the fibres of the micro-structured samples have been previously recrystallized in argon neutral atmosphere at 2000 °C for about 5 h. Preliminary tests were performed with two different oven container types,  $ZrO_2$  (Fig. 1 green coloured bars) and tungsten foil (Fig. 1 blue coloured bars), which did not show any significant influence on the fibres grain size at different temperatures and heating durations as shown on Fig. 1. SEM cross-sections were made on both samples (Fig. 3a and 3b). For each, about 2000 grains

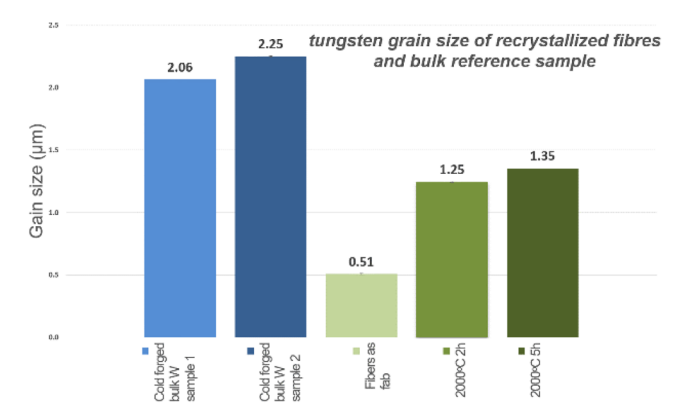


**Fig. 2.** Compared tungsten grain size of recrystallized fibres and bulk reference sample.

were sampled to find an average grain size of about 1.35  $\pm$  0.33  $\mu m$  (Fig. 2) (over 10 to 40  $\mu m$  in length, along fibre axis). This need to be compared to the original un-recrystallized fibres that displayed grains around 0.51  $\mu m$  (  $\pm$  0.06) (Fig. 2) and to the bulk reference cold forged tungsten, which has an average grain of 2.15  $\mu m$  with a standard deviation of 0.99  $\mu m$  (Fig. 2).

It has to be reminded that a first experimental demonstration of a 10<sup>5</sup> factor improvement for micro-structured tungsten over bulk 'ITERgrade' tungsten concerning ELM-like induced thermal fatigue was already made [9]. It was shown that even after 10<sup>5</sup> pulses at 0.5 GW/m<sup>2</sup>, micro-structured sample did not show any damage, unlike reference bulk sample that revealed some cracks even after a single pulse at such power density. The mechanism of this improvement was qualitatively explained within the same paper, however it was quantitatively evaluated, later, in [10] by means of finite element simulation (and by the same occasion re-tested), which also allowed to identify the physical mechanism behind. This mechanism is mainly the possibility of the material for free expansion owning to the gaps between the fibres in combination with a sufficiently small diameter of the fibres. This prevents to the build-up and accumulation of stress in material that results in damages like cracks or roughening. However, the production of a cold forged bulk tungsten bar, for the reference sample, and of extruded sub-millimetric fibres, for the micro-structured sample, strongly differs one to the other. Consequentially they offer significantly different grain structures and intrinsic different material properties, it could not be completely excluded that some of the improvement observed could also partially result from these material properties differences. This is why the current protocol has been implemented in order to bring the material grain microstructure of the two samples as close as possible to each other. Despite it, grains microstructure of fibres and bulk tungsten obviously hold differences (Fig. 2 and Fig. 3).

### 2.2. Experimental protocol

Experiment was performed at PSI-2 linear plasma facility [8]. At first, a deuterium plasma was applied for 150 min  $(3.42 \times 10^{25}\,\mathrm{D^+\,m^{-2}}$ , ion energy 41–62 eV, ~240 °C steady state) (Fig. 4). Additionally, a Nd:YAG laser (LASAG FLS 352 N) was used ( $\lambda=1064$  nm), with a pulse energy of 20 J (3.6 mm spot diameter, 1 ms pulse duration, 25 Hz pulse frequency) in order to simulate up to up to  $10^5$  ELM like pulses at 0.5 GW/m². It has to be noted, that unfortunately, laser broke down during experiment, after delivering  $10^5$  pulses to the micro-structured sample but only  $7\times10^4$  to the bulk tungsten reference sample. This protocol obviously has limitations like any others, but which are considered as limited as all samples are exposed to same conditions, and analysis and conclusion are drawn from comparison to each other's.

## 3. Experimental results

## 3.1. Thermal response

Temperatures during plasma irradiation as during laser fatigue tests were measured at the back of each sample with the help of two K-type thermocouple. Steady state temperature under  $D_2$  plasma was 244  $^{\circ}\text{C}$  for the micro-structured sample and 239  $^{\circ}\text{C}$  for the reference bulk tungsten sample at the beginning of the exposure.

Fig. 5 shows thermo-couples trace during the sequential exposure to deuterium plasma followed by the 10 batch of  $10^4$  laser pulses  $(0.5 \text{ GW/m}^2, 25 \text{ Hz}, 1 \text{ ms})$  on the micro-structured sample. This represents an average power density (in the laser Ø 3.6 mm spot area) of about 12.5 MW/m<sup>2</sup> for about 66 min, or 5.1 MW/m<sup>2</sup> when considering

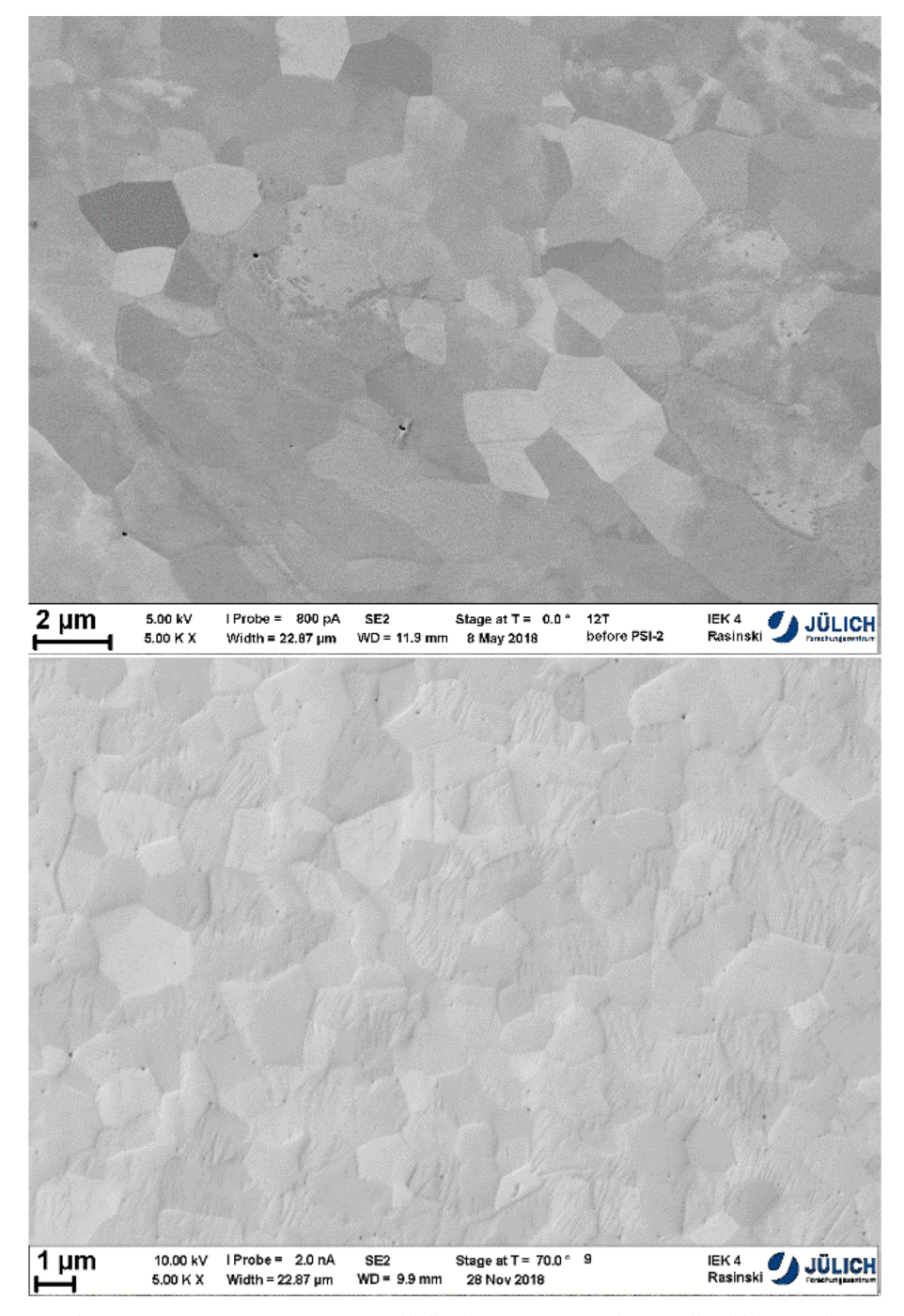


Fig. 3. Respective grain microstructure of bulk reference sample and recrystallized fibre sample.

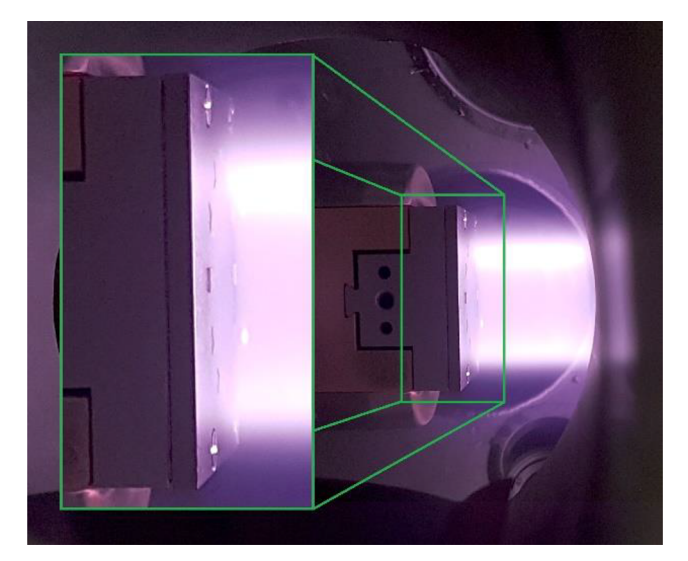
the whole front sample surface. It can be noticed that both samples display very similar temperatures during plasma irradiation despite being structurally different, which confirms the assumptions made in [9] about higher emissivity of the micro-structured sample. Same plasma load leads to same bottom surface temperature.

Meanwhile, during the transient phase, reference sample see its temperature increase, by a lower margin, by thermal conduction, as both sample are mounted on same holder with same mask. It has to be reminded that that this is a sequential load, and only the

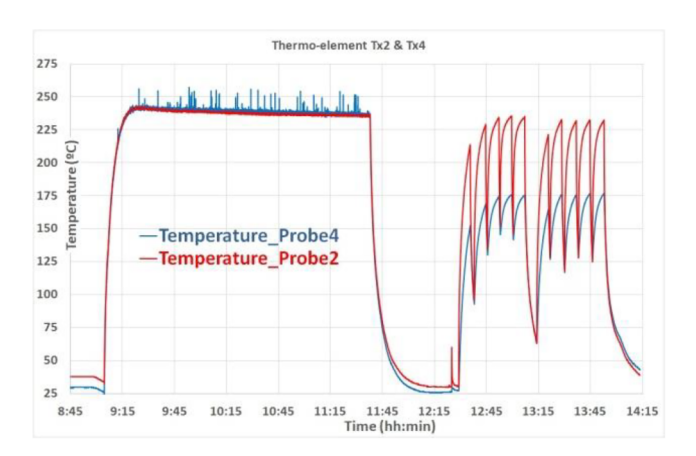
microstructured sample is loaded by laser, so temperature increase noticed on reference comes only from thermal conduction.

## 3.2. Sample damages

It is important to compare the damages that occurred on reference samples and the micro-structured sample made of recrystallized fibres. Fig. 6 clearly show the difference between samples damages that can be seen at macroscopic scales. It has to be noted that as already mentioned



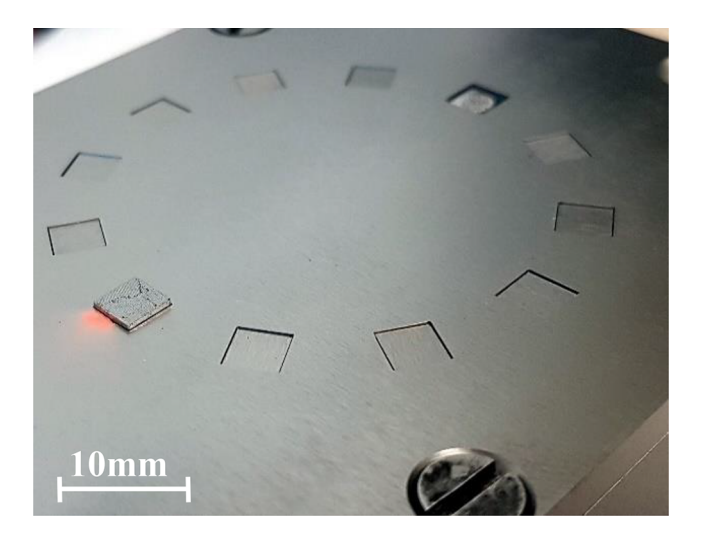
**Fig. 4.** Simultaneous plasma irradiation of both bulk tungsten sample (left) and of micro-structured sample (right).



**Fig. 5.** Thermo-couple traces of bulk tungsten reference sample (Tx4, blue) and of micro-structured sample (Tx2, green). (For interpretation of the references to colour in this figure legend, the reader is referred to the web version of this article.)

in [9] and [10], surface damage slightly increase absorption (< 20%) but with reduced influence which is why this it is not corrected in evaluations. It has to be noted that Fig. 6 top image shows that laser sublimated some of the underneath copper where fibres are embedded (due to laser incident angle of about 56 deg), which invalidated the results measured by gravimetric to quantify surface tungsten erosion. To spot further damages, a complete mapping of the front surface was made by means of optical microscopy at the resolution of 1  $\mu$ m/pixel, before (Fig. 7) and after (Fig. 8) the experiment. This revealed sufficient to track the appearance of cracks, roughness increase and material extrusion like observed in [10] but an additional complete SEM micrograph (resolution of 300 nm/pixel) was made to investigate the possible grain microstructure evolution (Fig. 9).

The difference is obvious regarding the amount of damage that each sample received. However, optical micrograph of micro-structured sample reveals that the combination of plasma and laser irradiation significantly removed interlayer of deposit that was present between



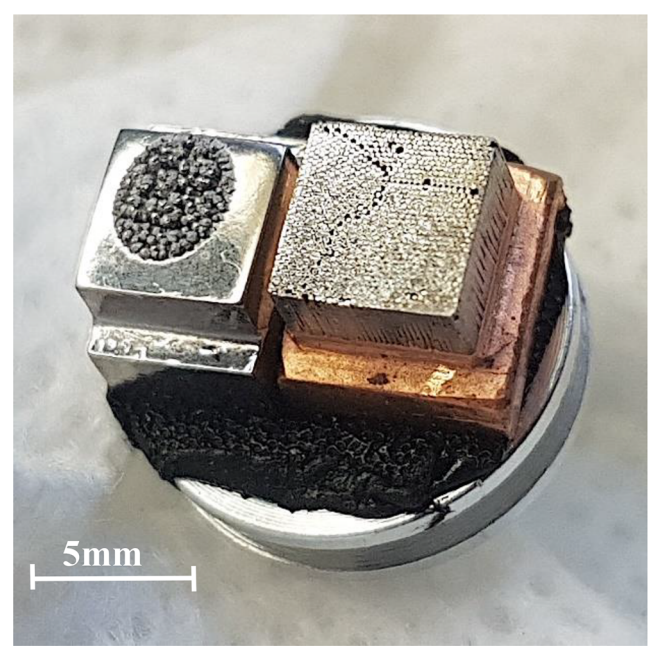


Fig. 6. Time traces of the surface temperature of micro-structured and reference tungsten samples and the laser power ( $\sim 10^4$  pulse).

fibres. This is believe to be electrolyte residue (from manufacturing sample) and/or oxide. Some cracks are also visible on single fibres; however they can be tracked back on the first micrograph, even if some could appear enlarged.

The SEM micrograph of reference sample (Fig. 9 bottom) reveals how strong are the damages, but without surprise, in line with [1,2,3] and [9,10], with extreme roughness increase and material extrusion. Meanwhile, micro-structured sample (Fig. 9 top), appears to be damage free. However, this SEM reveals several points, first, it confirms the mechanism that was explained within its concept [9] (micro-structuring PFM surface allows thermal expansion to happen without restriction, allows thermal cycling without secondary stress to build up and accumulate which leads to damages like cracks, roughening etc...), and, in addition, if the gaps between the fibres are too small, this mechanism cannot fully apply and may lead also to fibres damages. Fig. 10 is a good example of it, as thermal expansion results in the edge damages of

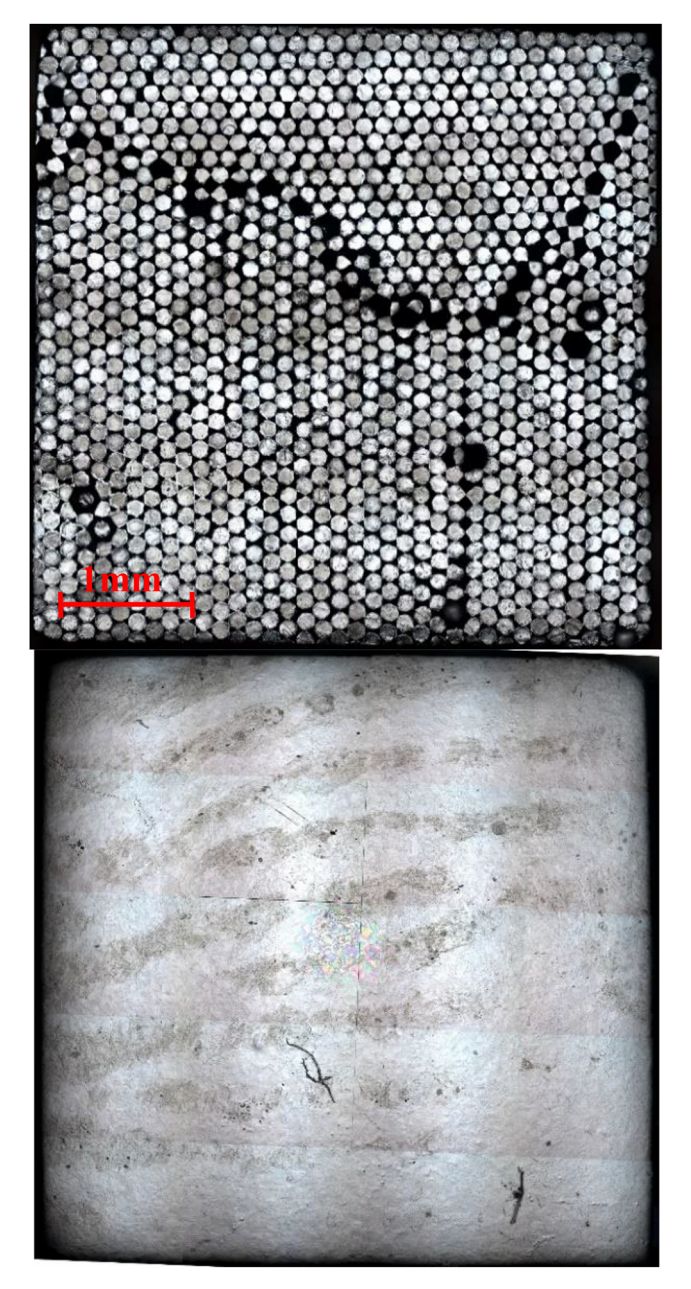


Fig. 7. Optical micrograph of the micro-structured and bulk samples before experiment.

fibres due to insufficient spacing. It can be observed that both or only one of the fibres in contact can be damaged, probably due to local hardness difference.

Fig. 10 also reveals the surface erosion, as we can still spot, electropolished surface (bottom left) that was prepared before experiment and newly eroded grain micro-structure that shows after experiment. This is also visible on Fig. 11, with bottom having kept almost its electro-polished surface, and top revealing eroded surface.

This brings up another aspect that was previously foreseen, that some fibres were delivered with inside cracks. This is very normal due to the wire drawing process that causes the tungsten to endure very high plastic deformation [11]. However, if these cracks are close

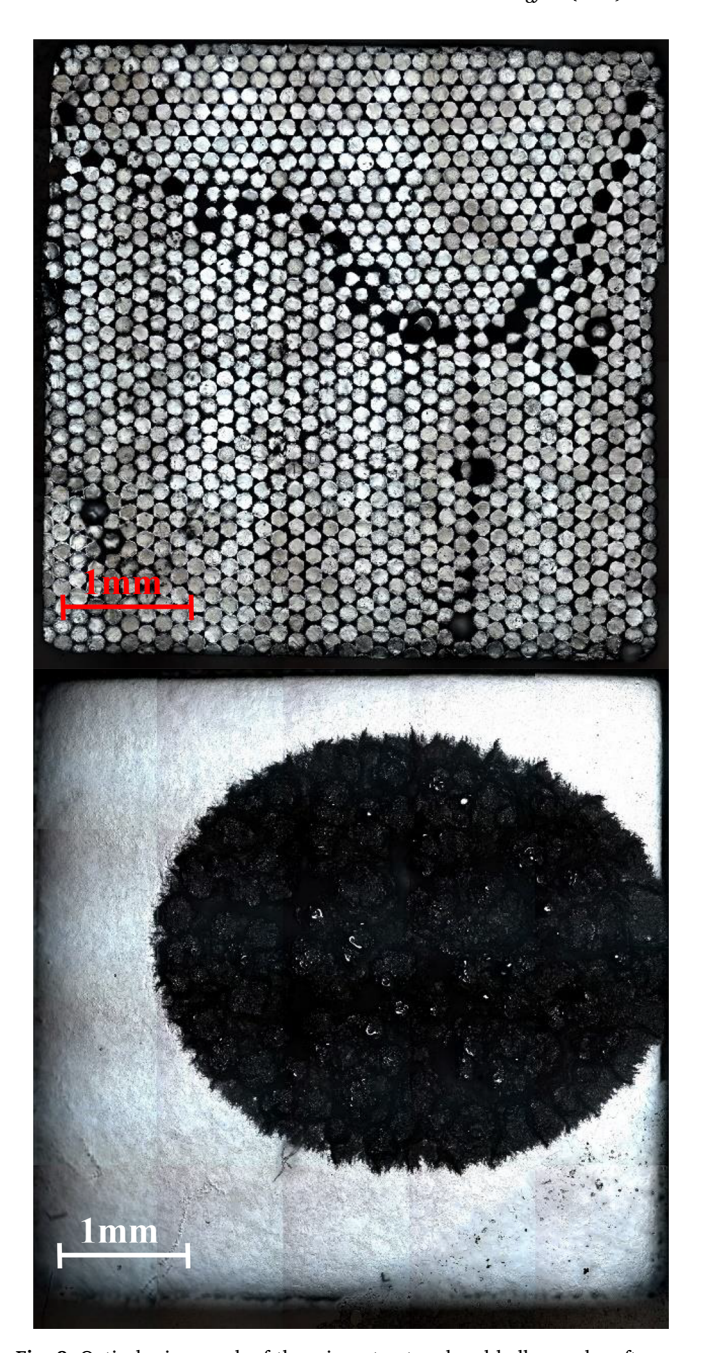


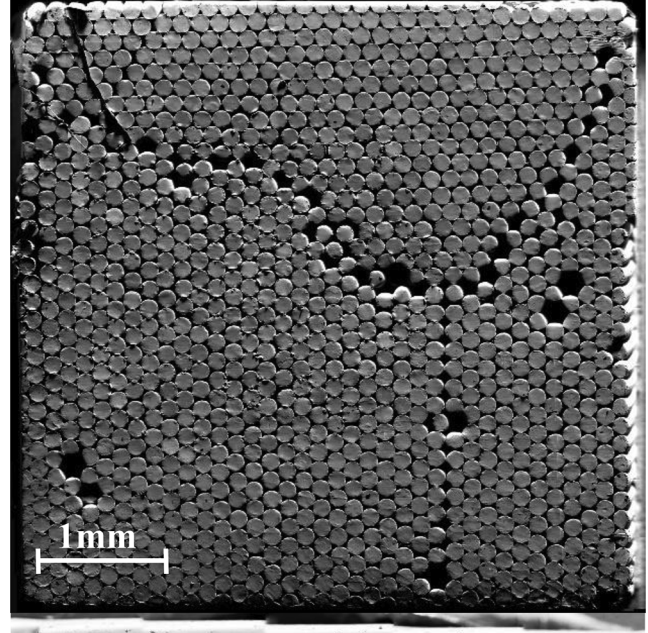
Fig. 8. Optical micrograph of the micro-structured and bulk samples after experiment.

enough to the surface, they can be revealed during the experiment, but from erosion of surface material, and not due to thermal stress (Fig. 11), and they could possibly lead to false positives (defect or damages).

This is also per this mechanism that the cracks can appear larger after plasma and laser irradiation.

## 4. Conclusions

Current paper is the occasion to confirm, with a different combination of plasma and laser irradiation, the results previously [9,10] observed concerning the ability of micro-structured tungsten to handle



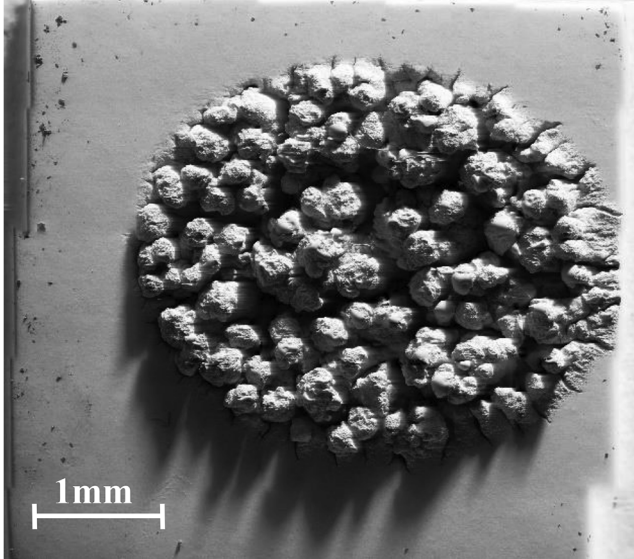


Fig. 9. SEM micrograph of the micro-structured and bulk samples after experiment.

very high ELM induced thermal fatigue. This is as much important as the value of this improvement factor being so high (confirmed  $10^5$  so far)

The mechanism of thermal fatigue resistance is highly independent of the mechanical properties of the fibre base tungsten material, therefore, the ability to withstand ELM will not be removed with PFC utilisation and possible recrystallization, but clearly comes from the design that was implemented. It cannot be totally excluded that material base properties, like ductility play a role within the ability to withstand thermal shocks, these seem to have a secondary role. This is reinforced as the manufacturing process of sample make great use of graphite (mould, guiding tools) which for sure contaminated the fibres, but also by the lower than DBTT steady state temperatures.

## CRediT authorship contribution statement

**A. Terra:** Conceptualization, Methodology, Software, Validation, Formal analysis, Investigation, Resources, Writing - original draft, Writing - review & editing, Visualization, Supervision, Project

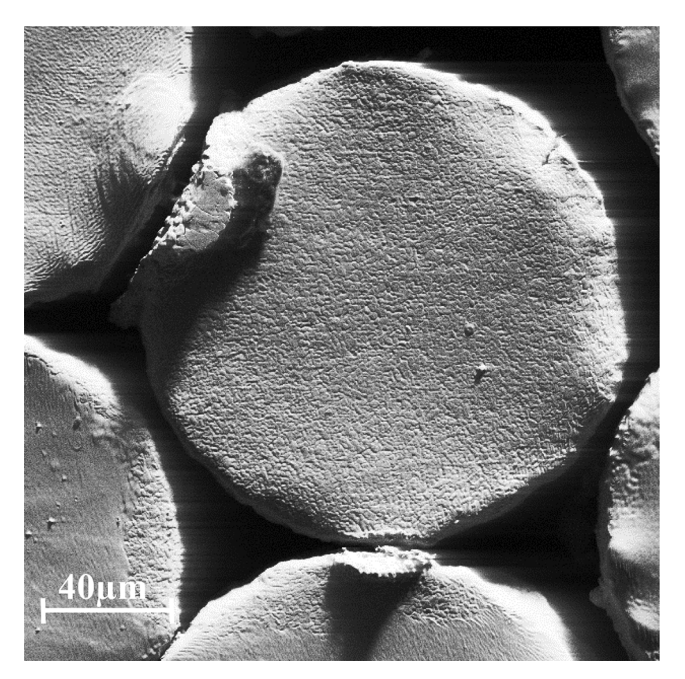


Fig. 10. SEM of insufficiently gapped fibres.

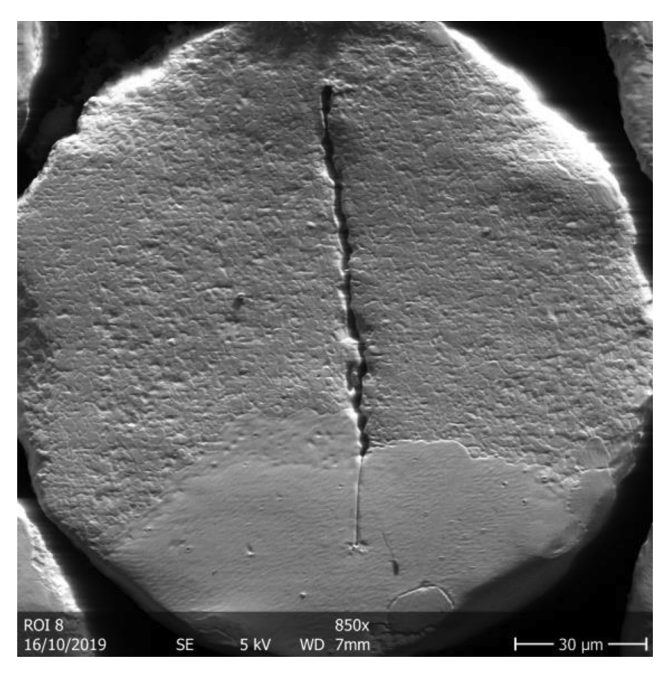


Fig. 11. SEM of an inner fibre eroded crack.

administration. G. Sergienko: Conceptualization, Methodology, Validation, Formal analysis, Investigation, Writing - original draft, Writing - review & editing, Visualization. A. Kreter: Methodology, Validation, Data curation. Y. Martynova: Conceptualization, Methodology, Validation. M. Rasiński: Methodology, Validation. M. Loewenhoff: Conceptualization, Methodology. Conceptualization, Methodology. G. Pintsuk: Methodology. D. Dorow-Gerspach: Methodology. Y. Mao: Conceptualization, Validation, Writing - review & editing. D. Schwalenberg: Conceptualization, Resources, Writing - review & editing. L. Raumann: Conceptualization, Writing - review & editing. J.W. Coenen: Funding acquisition, Resources, Writing - review & editing. S. Brezinsek: Data curation, Funding acquisition. B. Unterberg: Data curation, Funding acquisition. Ch. Linsmeier: Conceptualization, Funding acquisition.

#### **Declaration of Competing Interest**

The authors declare that they have no known competing financial interests or personal relationships that could have appeared to influence the work reported in this paper.

## Acknowledgements

A part of this work has been carried out within the framework of the EUROfusion Consortium (WP PFC) and has received funding from the Euratom research and training program 2014-2018 and 2019-2020 under grant agreement No. 633053. The views and options expressed herein do not necessarily reflect those of the European Commission.

### References

- Nygren, Richard E., Youchison, Dennis L. Mon. Testing of Tungsten and Tungsten-Armored Heat Sinks for Fusion Applications. United States. https://www.osti.gov/ servlets/purl/1142936.
- [2] T.h. Loewenhoff, S. Bardin, H. Greuner, J. Linke, H. Maier, T.W. Morgan, G. Pintsuk, R.A. Pitts, B. Riccardi, Impact of combined transient plasma/heat loads on tungsten performance below and above recrystallization temperature, Nucl. Fusion 55 (2015) 123004, https://doi.org/10.1088/0029-5515/55/12/123004.
- [3] M. Wirtz, A. Kreter, J. Linke, G. Th Loewenhoff, G.S. Pintsuk, I. Steudel, B. Unterberg, E. Wessel, High pulse number thermal shock tests on tungsten with steady state particle background, Phys. Scripta T170 (2017) 014066, https://doi. org/10.1088/1402-4896/ag909e.
- [4] C.h. Linsmeier, M. Rieth, J. Aktaa, T. Chikada, A. Hoffmann, J. Hoffmann, A. Houben, H. Kurishita, X. Jin, M. Li, Development of advanced high heat flux and plasma-facing materials, Nucl. Fusion 57 (2017) 092007, https://doi.org/10.

#### 1088/1741-4326/aa6f71.

- [5] J. Reiser, J. Hoffmann, M. Ute Jäntsch, S. Klimenkov, C. Bonk, A. Bonnekoh, T. Hoffmann, M.R. Mrotzek, Ductilisation of tungsten (W): On the increase of strength and room-temperature tensile ductility through cold-rolling, Int. J. Refract. Metals Hard Mater. 64 (2017) 261–278, https://doi.org/10.1016/j.ijrmhm.2016. 10.018
- [6] J. Reiser, L. Garrison, H. Greuner, J. Hoffmann, T. Weingärtner, U. Jäntsch, M. Klimenkov, P. Franke, S. Bonk, C. Bonnekoh, S. Sickinger, S. Baumgärtner, D. Bolich, M. Hoffmann, R. Ziegler, J. Konrad, J. Hohe, A. Hoffmann, T. Mrotzek, M. Seiss, M. Rieth, A. Möslang, Ductilisation of tungsten (W): Tungsten laminated composites, Int. J. Refract. Metals Hard Mater. 69 (2017) 66–109, https://doi.org/ 10.1016/j.jirmhm.2017.07.013.
- [7] J.W. Coenen, Y. Mao, S. Sistla, J. Riesch, T. Hoeschen, C.h. Broeckmann, R. Neu, C.h. Linsmeier, Improved pseudo-ductile behavior of powder metallurgical tungsten short fiber-reinforced tungsten (Wf/W), Nuclear Materials and Energy 15 (2018) 214–219, https://doi.org/10.1016/j.nme.2018.05.001.
- [8] A. Kreter, C. Brandt, A. Huber, S. Kraus, S. Moeller, M. Reinhart, B. Schweer, G. Sergienko, B. Unterberg, Linear plasma device PSI-2 for plasma-material interaction studies, Fusion Sci. Technol. 68 (1) (2015) 8–14, https://doi.org/10.13182/ FST14-906.
- [9] A. Terra, G. Sergienko, M. Tokar, D. Borodin, T. Dittmar, A. Huber, A. Kreter, Y. Martynova, S. Möller, M. Rasiński, M. Wirtz, Th. Loewenhoff, D. Dorow-Gerspach, Y. Yuan, S. Brezinsek, B. Unterberg, Ch. Linsmeier, Micro-structured tungsten; an advanced plasma-facing material, Nucl. Mater. Energy 19 (2019) 7–12, https://doi.org/10.1016/j.nme.2019.02.007.
- [10] A. Terra, G. Sergienko, M. Gago, A. Kreter, Y. Martynova, M. Rasiński, M. Wirtz, Th. Loewenhoff, Y. Mao, D. Schwalenberg, L. Raumann, J. W. Coenen, S. Moeller, Th. Koppitz, D. Dorow-Gerspach, S. Brezinsek, B. Unterberg, and Ch. Linsmeier, Microstructuring of tungsten for mitigation of ELM-like fatigue, Phys. Scripta Topical Issue T180, doi.org/10.1088/1402-4896/ab4e33.
- [11] P. Zhao, J. Riesch, T. Höschen, J. Almanstötter, M. Balden, J.W. Coenen, R. Himml, W. Pantleone, U. von Toussaintb, R. Neub, f, Microstructure, mechanical behaviour and fracture of pure tungsten wire after different heat treatments, Int. J. Refract. Metals Hard Mater. 68 (2017) 29–40, https://doi.org/10.1016/j.ijrmhm.2017.06.001.